# Dynamic Nuclear Polarization NMR: Overhauser Effect or Truncated Cross Effect?

Asif Equbal,<sup>†,§</sup> Yuanxin Li ,<sup>†,§</sup> Alisa Leavesley,<sup>†</sup> Shengdian Huang,<sup>‡</sup> Suchada Rajca,<sup>‡</sup> Andrzej Rajca,<sup>‡</sup> and Songi Han<sup>\*,†,¶</sup>

†Department of Chemistry and Biochemistry, University of California, Santa Barbara, Santa Barbara, California 93106, United States.

‡Department of Chemistry, University of Nebraska, Lincoln, Nebraska 68588-0304, United States.

¶Department of Chemical Engineering, University of California, Santa Barbara, Santa Barbara, California 93106, United States.

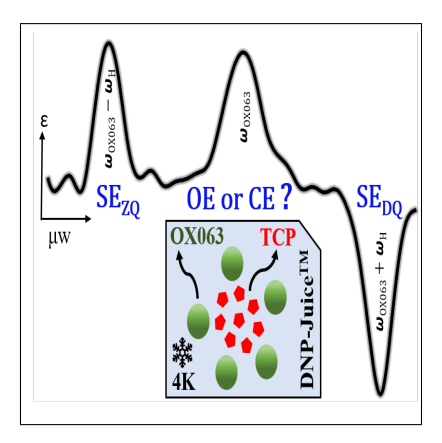
§Contributed equally to this work

E-mail: songi@chem.ucsb.edu

#### Abstract

This letter reports on the discovery of a truncated cross-effect in dynamic nuclear polarization (DNP) NMR that has the features of an Overhauser-effect DNP (OE-DNP). The apparent OE-DNP, where minimal microwave power achieved optimum enhancement, was observed when doping Trityl-OX063 with a nitroxide radical that possesses electron withdrawing, gem-dicarboxylate ester substitutes (TCP) in vitried water/glycerol at 6.9 Tesla and at 3.3 to 85 Kelvin, in apparent contradiction to expectations. While the observations are fully consistent with OE-DNP, we discover that a truncated cross-effect (CE) is the underlying mechanism, owing to TCP's shortened  $T_{1e}$ . We take this observation as a guideline, and demonstrate that a crossover from CE to apparent OE can be replicated by simulating CE of a narrow-line (Trityl-OX063) and a broad-line (TCP) radical pair, with a signicantly shortened  $T_{1e}$  of the broad-line radical.

### **Graphical TOC Entry**



Dynamic nuclear polarization (DNP) is the most important adjunct to nuclear magnetic resonance (NMR) to overcome its intrinsic insensitivity. <sup>1-6</sup> DNP enables magnetic resonance studies of a broad range of applications that would be infeasible otherwise, even at the highest magnetic field available today. DNP exploits microwave-induced polarization transfer from unpaired electrons to nuclear spins, while three distinct DNP mechanisms are of main relevance: solid effect (SE), cross effect (CE), and Overhauser effect (OE). Of these DNP mechanisms, SE and OE are straightforward to conceptualize, as they involve the direct transfer of polarization from an electron to a hyperfine-coupled nucleus. The optimal SE condition requires microwave ( $\mu$ w) irradiation at the forbidden electron-nuclear (e-n) double-quantum (DQ) and zero-quantum (ZQ) transitions. <sup>7,8</sup> The condition for OE is very different in that it requires  $\mu$ w irradiation at the allowed single-quantum (SQ) transition as well as spin-dynamics that render the e-n ZQ and DQ cross-relaxation rates different. The CE mechanism involves two coupled electrons for transferring polarization to an unequally coupled nucleus. 9-12 The CE condition in an e-e-n spin system is fulfilled when the difference in the resonance frequencies of the two electron spins equals the nuclear Larmor frequency.

An important focus in DNP has been on optimizing the paramagnetic polarizing agent and solvent to yield maximum DNP enhancements.  $^{13-20}$  However, a rational understanding of the effect of the properties of the radical or radical mixture, solvent, temperature, and magnetic field on the DNP efficiency and mechanism is still elusive. The SE and CE are the most prominent DNP mechanisms in non-conducting solid-state samples. In contrast, the OE mechanism has been thought to be relevant only in conducting-solids or liquids where electron spin diffusion and molecular tumbling motion can provide rapidly fluctuating hyperfine couplings, causing efficient e-n ZQ or DQ cross-relaxation.  $^{1,2}$  However, contrary to expectations, Can et. al.  $^{21}$  recently reported on an unexpected observation of OE with the non-conducting, narrow line, polarizing agent, 1,3-bisdiphenylene-2-phenylallyl (BDPA)  $^{22}$  dispersed in polystyrene and with sulfonated-BDPA (SA-BDPA)  $^{23}$  in a glassy

glycerol/ $H_2O/D_2O$  (6:3:1) matrix termed DNP-juice<sup>TM</sup>, at 100 K and an external magnetic field between 5 T and 18.8 T. This discovery of OE in insulating solids is considered pivotal for the prospect of DNP in high magnetic fields, owing to the low microwave power requirement of OE and the potential field-independence of the DNP efficiency. However there are two important challenges in further exploring the potential of OE in the study of bio-solids: (i) the OE polarizing agent, BDPA, is incompatible with biological samples. (ii) the mechanistic basis for the OE in insulating solids is unclear because the underlying relaxation mechanism is unknown in insulating solids. This makes the discovery of OE in insulating solids by Can et. al. unexpected and exciting. Even more curiously, reports of OE-DNP mechanism in non-conducting SA-BDPA have been made by Bodenhausen and coworkers at temperatures as low as 1.2K under static conditions and at 6.7 T<sup>24</sup>, while there is no obvious physical basis for the occurrence of fast e - n fluctuations near the electron Larmor frequency under these experimental conditions. Recent work by Pylaeva et. al. 25 discusses possible mechanisms for the observed OE in BDPA on the basis of molecular dynamics and spin dynamics simulations, but a rigorous experimental proof does not exist to date.

Counter to the proposed theory<sup>25</sup> and our own expectations, we observed a very similar strong OE features with Trityl-OX063 (OX063) when doped with equivalent amounts of tetracarboxylate-ester-pyrroline (TCP) nitroxide radicals<sup>26</sup> across a wide range of temperatures in DNP-juice<sup>TM</sup>. This intriguing discovery further showed that varying the solvent from DNP-juice<sup>TM</sup> to DMSO not only changes the DNP efficiency, but also the apparent DNP mechanism from OE to CE in hitherto unknown ways. This letter reports on a series of experiments and quantum mechanical calculations of the DNP mechanism that yield a rationale basis for the apparent OE observed with OX063-TCP mixtures in DNP-juice<sup>TM</sup>. The structures of OX063 and TCP radicals investigated here are shown in SI. TCP has two forms, TCP1 and TCP2. After confirming that both display similar EPR parameters, as well as similar DNP properties (see SI), we chose to focus on presenting results on only TCP2.

The DNP frequency-profile is indicative of the underlying DNP mechanism and the opti-

mum conditions.  $^{6,9,27-29}$  Figure 1 (a) shows the DNP frequency-profile of a mixture containing 15 mM TCP2 and 15 mM OX063 dissolved in DNP-juice<sup>TM</sup> at 4 K. Significant <sup>1</sup>H DNP enhancements were observed at the  $\mu$ w irradiation frequencies of  $\sim$ 193.3 GHz,  $\sim$ 193.6 GHz and  $\sim$ 193.9 GHz. Clearly, the enhancements at 193.3 GHz and 193.9 GHz are  $\pm$ 300 MHz apart from the OX063 center-frequency, and correspond to conditions for SE<sub>ZQ</sub> and SE<sub>DQ</sub> DNP, respectively. The enhancement at 193.6 GHz was a priori assigned to OE as it corresponds to OX063's center-frequency at 6.9 T. Observing OE around this frequency was not only unexpected, but also initially inexplicable, and therefore will be denoted as OE\*, with the \* marking an apparent OE. Surprisingly, no visible features of TCP2 in DNP-juice<sup>TM</sup> appeared in the observed frequency-profile.

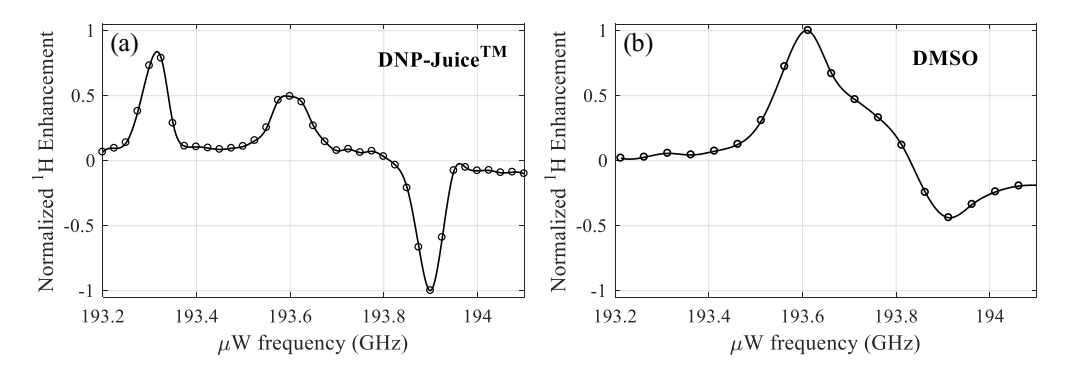


Figure 1: DNP frequency profiles of 15mM TCP2 - 15mM OX063 mixture in (a) DNP juice<sup>TM</sup> at 4K; (b) DMSO/D<sub>2</sub>O at 4K. DNP frequency-profiles were obtained by measuring <sup>1</sup>H DNP signal enhancement as a function of  $\mu$ w irradiation frequency which was swept from 193.2 GHz to 194.1 GHz, with 120 mW  $\mu$ w-power and 60s irradiation time. The <sup>1</sup>H enhancements displayed were normalized by the maximum value in the graph.

The DNP frequency-profile was also measured for the same OX063-TCP2 mixture in DMSO. Adding to the OE\* conundrum, the frequency-profile in DMSO displayed a diametrically different frequency envelope, revealing a dominant CE DNP mechanism. The positive and the negative maximum enhancements were observed at ~193.6 GHz and ~193.9 GHz, respectively (Figure 1 (b)). The separation of these maximum peak positions by 300 MHz is consistent with CE between OX063 and TCP2, while the broader features are presumably due to operational CE between two TCP2 radicals, where a range of electron spin pairs at

different  $\mu$ w-frequencies fulfill the CE conditions. The presence of the OE\* mechanism in DMSO cannot be ruled out, since the optimum frequency for the OE\* (observed in DNP-juice<sup>TM</sup>) coincides with the peak resulting from TCP2-OX063 CE. At the center frequency of 193.6 GHz for optimum OE\*, enhancements (signal intensity ratio:  $\mu w_{on}/\mu w_{off}$ ) of ~31 was observed for TCP2-OX063 in DNP-juice<sup>TM</sup> and ~139 in DMSO, both at 4K with 120 mW  $\mu$ w-power and 60 s irradiation.

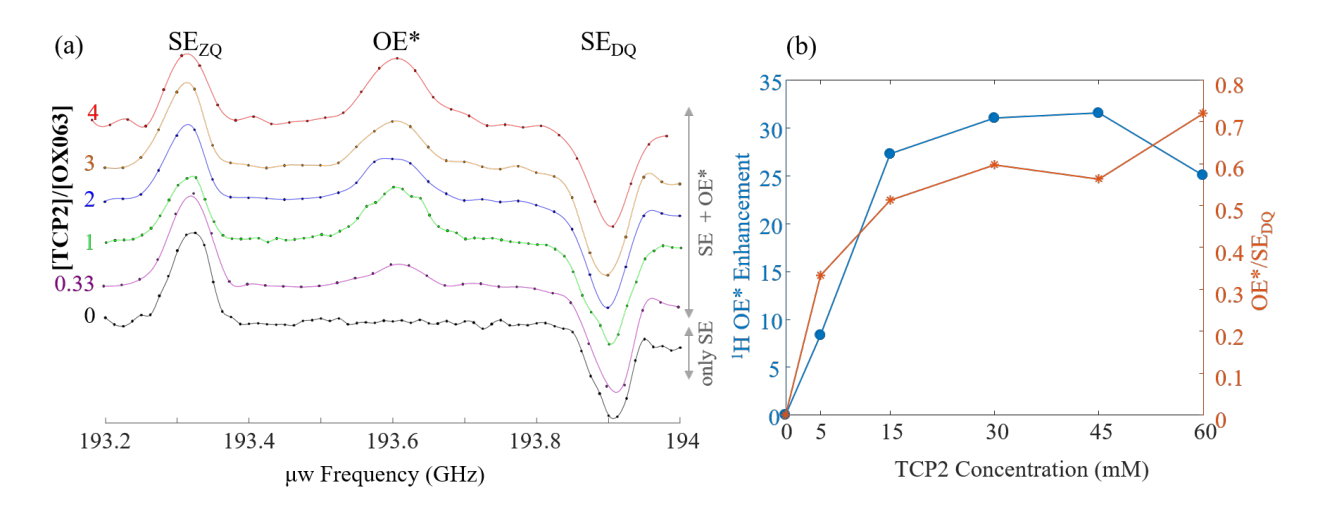


Figure 2: (a)TCP2:OX063 ratio optimization for maximum OE\* enhancement at 4K in DNP-juice  $^{TM}$  using:  $\mu$ w irradiation time,  $T_B=60$  s and  $\mu$ w-power = 120 mW. OX063 concentration was fixed to 15mM. All the profiles are normalized with corresponding  $SE_{DQ}$  enhancement number. (b) Absolute OE\* enhancement on the left y-axis and OE\*/ $SE_{DQ}$  ratio on the right y-axis for different radical concentrations.

Next, we investigate the radical mixture composition to achieve optimum  $OE^*$  enhancements in DNP-juice<sup>TM</sup> (at 4K, 120 mW  $\mu$ w power, 60 s irradiation time). We recorded the DNP frequency-profile of a series of TCP2/OX063 mixtures, where the OX063 concentration was fixed at 15 mM and the TCP2 concentration varied from 0 to 60 mM (Figure 2 (a)). All frequency-profiles were normalized with respect to the optimum  $SE_{DQ}$  enhancement. The DNP frequency-profile shows  $OE^*$  enhancements only with TCP2 doping, in addition to SE enhancements at 193.3 and 193.9 GHz. The absolute  $OE^*$  enhancement and its relative efficiency with respect to  $SE_{DQ}$ ,  $OE/SE_{DQ}$ , are plotted in Figure 2 (b). They show that an increase in the TCP2 concentration leads to an increase in the  $OE^*$  enhancement up to 30

mM, after which it plateaus with increasing TCP2 concentration (and slightly decreases at 60 mM). For all the following investigations, the radical mixture composition was fixed to the optimum composition of 15 mM OX063 and 30 mM TCP2.

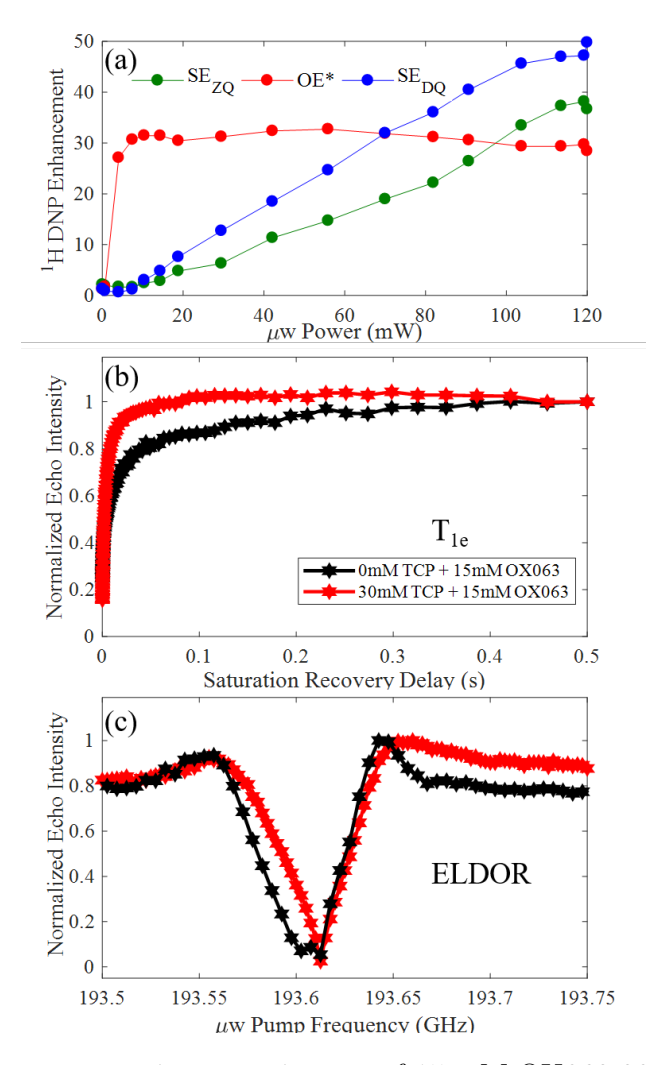


Figure 3: (a) DNP power saturation experiments of 15 mM OX063 30 mM TCP2 mixture in DNP-juice<sup>TM</sup> were recorded with  $\mu$ w-power varied from 0 to 120 mW with 60 s T<sub>B</sub>. (a) was recorded at 4K and  $\mu$ w-frequency was fixed at the optimum condition of SE<sub>ZQ</sub> (green), OE\* (red) and SE<sub>DQ</sub> (blue), respectively. (b) <sup>1</sup>H OE\* enhancement was recorded as a function of temperature (from 3.3 K to 85 K) with 120 mW  $\mu$ w-frequency at 193.6125 GHz and T<sub>B</sub> of 60s. (c) T<sub>1e</sub> of pure OX063 (black) and TCP2-doped OX063 (red). (d) ELDOR experiments of pure OX063 (black) and TCP2-doped OX063 (red).

The DNP power-curve (enhancement vs.  $\mu$ w power) at the OE\* frequency showed that the maximum enhancement (at a fixed 60-s irradiation time) was reached at merely 7 mW of  $\mu$ w power, as shown in Figure 3 (a). Remarkably, 90% of the maximum enhancement was

achieved with minuscule (4 mW)  $\mu$ w power, further corroborating the signature properties of OE. In stark contrast, the optimum power for SE-DNP enhancements could not be met by even at 120mW of  $\mu$ w-power. At low  $\mu$ w power, the OE\*-derived enhancement was higher by as much as 16-fold compared to the SE-derived enhancements. At higher  $\mu$ w power (>70 mW), the SE started to dominate over the OE\* (at 4K). Impressively, the low power requirement to saturate the OE\* resonance was observed even at higher temperatures of 10 K and 25 K, and at low TCP2 concentrations (5 mM), indicating that the OE\* effect is not power-limited under the tested conditions (shown in SI). Further adding to OE\*'s advantage, the polarization buildup rate for OE\* was found to be faster than for the SE (see SI). The temperature dependence showed a surprisingly sharp increase in OE\* enhancement below 5 K (see SI), indicating the pivotal role of electron relaxation in the OE\* phenomenon, given that saturation can be ruled out as a limiting factor.

We compare our results with reported OE studies of BDPA in the literature. Can et. al. attributed the absence of OE in OX063 and perdeuterated BDPA ( $d_{21}$ -BDPA) to the absence of strong (e-n) couplings<sup>21</sup>. In our case, OX063, all hydrogen atoms in the aromatic rings joined directly to the carbon radical center are purposefully substituted to remove the influence of large e-H hyperfine-couplings.<sup>14</sup> The study by Pylaeva et. al.<sup>25</sup> furthermore proposed that fluctuation in the electron spin density in BDPA owing to conjugation in the carbon radical position can lead to hyperfine-couplings fluctuations. Ji et. al.<sup>24</sup> hypothesized that stochastic motions at low vibration frequencies can be a source of non-zero spectral density at the electron resonance frequency leading to cross-relaxation, effective at low temperatures. Hyperfine-coupling fluctuations due to conjugation would not be a plausible mechanism for OX063, as the radical carbon position is fixed in OX063. Therefore, OX063 does not meet any of the hypothesized requirements (strong e-n coupling and conjugation) for exhibiting OE in the pure or doped state. Equally peculiar is our observation that OE\* is turned on/off with the choice of the glassing solvent. Although the results du-

plicate the apparent properties of OE-DNP observed in insulating solids, it does not meet the theoretical basis.

Solving this OE\* riddle requires scrutiny of the electron spin dynamics. This was enabled with unique instrumentation, which allowed for the measurement of the EPR signal, polarization-profile, and relaxation times under the relevant DNP conditions. The echodetected  $T_{1e}$  relaxation rates were measured at the frequencies corresponding to the OE\* and SE transitions. The  $T_{1e}$  of pure OX063 in DNP-juice<sup>TM</sup> was found to be ~16 ms, which shortened to ~4 ms upon addition of 30 mM TCP2 (Figure 3(b)). Crucially, the  $T_{1e}$  of TCP2 in DNP-juice<sup>TM</sup> was too short () to be detected (also attributed to very short  $T_m$ ), while  $T_{1e}$  of TCP2 in DMSO was significantly longer (  $\approx 17$  ms), and therefore easily detectable by pulsed EPR. This hints at clustering  $^{31,32}$  of TCP2 in DNP-juice  $^{TM}$ . This was confirmed by CW X-band EPR that shows signature of dipolar brodening for TCP2 in DNP-juice  $^{TM}$ , but not in DMSO (see SI). That the  $T_{1e}$  of OX063 and/or nitroxide radicals be so critically solvent and mixture-dependent was unexpected, showcasing the need to evaluate  $T_{1e}$  at the precise experimental DNP conditions. Tabulated  $T_{1e}$  values and further discussions on  $T_{1e}$  with respect to literature can be found in the SI.

Further insight was gained with electron-electron double resonance (ELDOR) that measured how EPR saturation or polarization at one frequency is transferred to another frequency. In the ELDOR-profile shown in Figure 3 (c), the electron detection/probe frequency was set to that of the OX063 center, and the saturating/pump frequency scanned from 193.5 to 193.75 GHz with 120 mW power at 4K. The ELDOR-profile showed that  $\mu$ w-irradiation resonant with TCP2 did not affect the OX063 resonance. This is consistent with the very fast relaxation of TCP2 in DNP-juice<sup>TM</sup> that is hence not saturable. Also, the hole burnt at the OX063 frequency narrows upon addition of TCP2, consistent with the shortening of OX063's  $T_{1e}$  upon doping with TCP2, especially with clustered TCP2 in DNP-juice<sup>TM</sup>.

Inspired by the observed EPR results, we quantum mechanically simulated the DNP frequency-profile for a narrow radical ( $e_1$ -OX063) and a broad radical ( $e_2$ -TCP2), differently

coupled to a proton in an  $e_1 - e_2$ -H system. Mimicking the slow-fast relaxation rates combination in DNP-juice<sup>TM</sup>,  $T_{1e}$  of  $e_1$  and  $e_2$  were set to 0.01 and 4 ms, respectively. The DNP simulation was performed using Spin Evolution, a software package for spin dynamics simulations.  $^{33}$  All relevant details of the simulation is provided in the SI. Remarkably, we could replicate the experimental <sup>1</sup>H enhancement frequency-profile of OX063-TCP2 mixture. A positive maximum enhancement is observed at the OX063 center-frequency, as well as  $\pm 300$ MHz apart from the OX063 center, representing the  $SE_{ZQ}$  and  $SE_{DQ}$  conditions. Clearly, the OE\* feature is observed, even though the cross-relaxation mechanisms are turned off, i.e. the mechanistic prerequisites for the OE eliminated. This shows that the observed OE\* is nothing but a truncated CE induced by conditions when one of the two electron spins involved in the CE has a very short  $T_{1e}$ . The CE relies on the selective saturation of one of the coupled electron spins. Thus, irradiation of the slower relaxing, "easy to saturate", electron spin (e<sub>1</sub>) (Fig. 4(b)) will lead to an effective polarization transfer to the nucleus. In contrast, irradiation of the very fast relaxing electron spin  $(e_2)$  will not result in electron saturation, and thus no appreciable polarization differential. Consequently, the CE polarization transfer will be truncated at the EPR frequencies of the fast relaxing radical, TCP2 in this study. The simulated power-profile also mimics the experimental result as shown in SI.

In summary, this letter reports on the discovery of a truncated cross effect that has the appearance of an Overhauser DNP effect. Such an effect was observed when doping OX063 with the nitroxide based radical, TCP2, in vitrified water/glycerol. The mechanistic basis for this astonishing effect was found to be a substructure of the CE mechanism defined by distinct electron spin dynamics properties. The puzzling  $OE^*$  mechanism can be replicated by quantum mechanical simulations with a mixed radical system, where the two radicals maximize the EPR spectral overlap to fulfill the CE conditions, while one radical type is easily saturated, but not the other, due to very short  $T_{1e}$ . This discovery is potentially important in many different ways, one of which is the prospect of the truncated CE serving

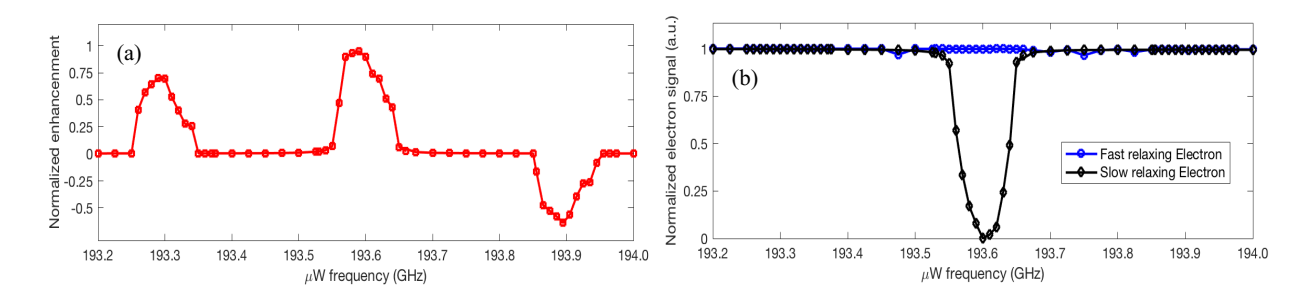


Figure 4: (a)Simulated <sup>1</sup>H DNP enhancement as a function of  $\mu$ w irradiation frequency, for a eeH spin system at 300 MHz conditions. (b) Polarization measurements of the two electrons under the DNP conditions of figure 1 a. This is demonstrated using a three spins (two electrons and one proton) based simulation at the experimental condition taken of figure 1. The longitudinal relaxation rate constants of electrons are taken to be 0.01 and 4 ms, mimicking relaxation rates of TCP2 and OX063, respectively. All the other simulation parameters are mentioned in the supporting information.

as an indirect read out of "dark" (or invisible) electron spins that, despite being undetectable, elicit a truncated CE by means of a detectable reporter radical. The OE characteristics may be a spurious effect owing to its similarity with the truncated CE, and therefore, in general probing electron-spins dynamics will be the ultimate test of the underlying mechanism, and not just the DNP profiles.

### Acknowledgement

This work was supported by the National Science Foundation (NSF) (CHE #1505038 to SH and #CHE-1665256 to AR) and the National Institute of Health (NIH) (NIBIB #1R21EB022731 to SH and NIGMS #R01GM124310-01 to SR and AR). The content is solely the responsibility of the authors and does not necessarily represent the official views of the National Institutes of Health.

## **Supporting Information**

The supporting information is available free of charge on the ACS publication website at DOI: XXX.

#### References

- (1) Overhauser, A. W. Polarization of nuclei in metals. *Physical Review* **1953**, *92*, 411.
- (2) Carver, T. R.; Slichter, C. P. Polarization of nuclear spins in metals. *Physical Review* 1953, 92, 212.
- (3) Wind, R.; Duijvestijn, M.; Van Der Lugt, C.; Manenschijn, A.; Vriend, J. Applications of dynamic nuclear polarization in 13C NMR in solids. *Progress in Nuclear Magnetic Resonance Spectroscopy* **1985**, *17*, 33–67.
- (4) Ardenkjær-Larsen, J. H.; Fridlund, B.; Gram, A.; Hansson, G.; Hansson, L.; Lerche, M. H.; Servin, R.; Thaning, M.; Golman, K. Increase in signal-to-noise ratio of> 10,000 times in liquid-state NMR. Proceedings of the National Academy of Sciences 2003, 100, 10158–10163.
- (5) Ardenkjaer-Larsen, J.-H.; Boebinger, G. S.; Comment, A.; Duckett, S.; Edison, A. S.; Engelke, F.; Griesinger, C.; Griffin, R. G.; Hilty, C.; Maeda, H. et al. Facing and overcoming sensitivity challenges in biomolecular NMR spectroscopy. *Angewandte Chemie International Edition* 2015, 54, 9162–9185.
- (6) Thankamony, A. S. L.; Wittmann, J. J.; Kaushik, M.; Corzilius, B. Dynamic nuclear polarization for sensitivity enhancement in modern solid-state NMR. Progress in Nuclear Magnetic Resonance Spectroscopy 2017, 102-103, 120 195.
- (7) Jeffries, C. Polarization of nuclei by resonance saturation in paramagnetic crystals. *Physical Review* **1957**, *106*, 164.
- (8) Hovav, Y.; Feintuch, A.; Vega, S. Theoretical aspects of dynamic nuclear polarization in the solid state—the solid effect. *Journal of Magnetic Resonance* **2010**, *207*, 176–189.
- (9) Hwang, C. F.; Hill, D. A. Phenomenological model for the new effect in dynamic polarization. *Physical Review Letters* **1967**, *19*, 1011.

- (10) Hovav, Y.; Feintuch, A.; Vega, S. Theoretical aspects of dynamic nuclear polarization in the solid state—the cross effect. *Journal of Magnetic Resonance* **2012**, *214*, 29–41.
- (11) Thurber, K. R.; Tycko, R. Theory for cross effect dynamic nuclear polarization under magic-angle spinning in solid state nuclear magnetic resonance: the importance of level crossings. The Journal of chemical physics 2012, 137, 084508.
- (12) Mentink-Vigier, F.; Akbey, Ü.; Oschkinat, H.; Vega, S.; Feintuch, A. Theoretical aspects of magic angle spinning-dynamic nuclear polarization. *Journal of Magnetic Resonance* **2015**, *258*, 102–120.
- (13) Song, C.; Hu, K.-N.; Joo, C.-G.; Swager, T. M.; Griffin, R. G. TOTAPOL: a biradical polarizing agent for dynamic nuclear polarization experiments in aqueous media. *Journal of the American Chemical Society* 2006, 128, 11385–11390.
- (14) Hu, K.-N.; Bajaj, V. S.; Rosay, M.; Griffin, R. G. High-frequency dynamic nuclear polarization using mixtures of TEMPO and trityl radicals. *The Journal of chemical* physics 2007, 126, 044512.
- (15) Zagdoun, A.; Rossini, A. J.; Gajan, D.; Bourdolle, A.; Ouari, O.; Rosay, M.; Maas, W. E.; Tordo, P.; Lelli, M.; Emsley, L. et al. Non-aqueous solvents for DNP surface enhanced NMR spectroscopy. *Chemical Communications* 2012, 48, 654–656.
- (16) Zagdoun, A.; Casano, G.; Ouari, O.; Lapadula, G.; Rossini, A. J.; Lelli, M.; Baffert, M.; Gajan, D.; Veyre, L.; Maas, W. E. et al. A slowly relaxing rigid biradical for efficient dynamic nuclear polarization surface-enhanced NMR spectroscopy: expeditious characterization of functional group manipulation in hybrid materials. *Journal of the American Chemical Society* 2012, 134, 2284–2291.
- (17) Sauvée, C.; Rosay, M.; Casano, G.; Aussenac, F.; Weber, R. T.; Ouari, O.; Tordo, P. Highly Efficient, Water-Soluble Polarizing Agents for Dynamic Nuclear Polarization at High Frequency. *Angewandte Chemie International Edition* **2013**, *52*, 10858–10861.

- (18) Mathies, G.; Caporini, M. A.; Michaelis, V. K.; Liu, Y.; Hu, K.-N.; Mance, D.; Zweier, J. L.; Rosay, M.; Baldus, M.; Griffin, R. G. Efficient dynamic nuclear polarization at 800 MHz/527 GHz with trityl-nitroxide biradicals. *Angewandte Chemie International Edition* 2015, 54, 11770–11774.
- (19) Kubicki, D. J.; Casano, G.; Schwarzwälder, M.; Abel, S.; Sauvée, C.; Ganesan, K.; Yulikov, M.; Rossini, A. J.; Jeschke, G.; Copéret, C. et al. Rational design of dinitroxide biradicals for efficient cross-effect dynamic nuclear polarization. *Chemical Science* 2016, 7, 550–558.
- (20) Perras, F. A.; Reinig, R. R.; Slowing, I. I.; Sadow, A. D.; Pruski, M. Effects of biradical deuteration on the performance of DNP: towards better performing polarizing agents. *Physical Chemistry Chemical Physics* **2016**, *18*, 65–69.
- (21) Can, T. V.; Caporini, M. A.; Mentink-Vigier, F.; Corzilius, B.; Walish, J. J.; Rosay, M.; Maas, W. E.; Baldus, M.; Vega, S.; Swager, T. M. et al. Overhauser effects in insulating solids. The Journal of Chemical Physics 2014, 141, 064202.
- (22) Koelsch, C. F. Syntheses with Triarylvinylmagnesium Bromides., -Bisdiphenylene-phenylallyl, a Stable Free Radical. *Journal of the American Chemical Society* **1957**, 79, 4439–4441.
- (23) Haze, O.; Corzilius, B.; Smith, A. A.; Griffin, R. G.; Swager, T. M. Water-Soluble Narrow-Line Radicals for Dynamic Nuclear Polarization. *Journal of the American Chemical Society* 2012, 134, 14287–14290, PMID: 22917088.
- (24) Ji, X.; Can, T.; Mentink-Vigier, F.; Bornet, A.; Milani, J.; Vuichoud, B.; Caporini, M.; Griffin, R.; Jannin, S.; Goldman, M. et al. Overhauser effects in non-conducting solids at 1.2K. *Journal of Magnetic Resonance* **2018**, *286*, 138 142.
- (25) Pylaeva, S.; Ivanov, K. L.; Baldus, M.; Sebastiani, D.; Elgabarty, H. Molecular Mecha-

- nism of Overhauser Dynamic Nuclear Polarization in Insulating Solids. *The Journal of Physical Chemistry Letters* **2017**, *8*, 2137–2142, PMID: 28445055.
- (26) Huang, S.; Paletta, J. T.; Elajaili, H.; Huber, K.; Pink, M.; Rajca, S.; Eaton, G. R.; Eaton, S. S.; Rajca, A. Synthesis and Electron Spin Relaxation of Tetracarboxylate Pyrroline Nitroxides. The Journal of Organic Chemistry 2017, 82, 1538–1544, PMID: 28032758.
- (27) Banerjee, D.; Shimon, D.; Feintuch, A.; Vega, S.; Goldfarb, D. The interplay between the solid effect and the cross effect mechanisms in solid state 13C DNP at 95 GHz using trityl radicals. *Journal of Magnetic Resonance* **2013**, *230*, 212–219.
- (28) Ravera, E.; Shimon, D.; Feintuch, A.; Goldfarb, D.; Vega, S.; Flori, A.; Luchinat, C.; Menichetti, L.; Parigi, G. The effect of Gd on trityl-based dynamic nuclear polarisation in solids. *Physical Chemistry Chemical Physics* 2015, 17, 26969–26978.
- (29) Leavesley, A.; Shimon, D.; Siaw, T. A.; Feintuch, A.; Goldfarb, D.; Vega, S.; Kaminker, I.; Han, S. Effect of electron spectral diffusion on static dynamic nuclear polarization at 7 Tesla. Physical Chemistry Chemical Physics 2017, 19, 3596–3605.
- (30) Siaw, T. A.; Fehr, M.; Lund, A.; Latimer, A.; Walker, S. A.; Edwards, D. T.; Han, S.-I. Effect of electron spin dynamics on solid-state dynamic nuclear polarization performance. *Physical Chemistry Chemical Physics* **2014**, *16*, 18694–18706.
- (31) Olankitwanit, A.; Kathirvelu, V.; Rajca, S.; Eaton, G. R.; Eaton, S. S.; Rajca, A. Calix [4] arene nitroxide tetraradical and octaradical. *Chemical Communications* **2011**, 47, 6443–6445.
- (32) Sato, H.; Kathirvelu, V.; Spagnol, G.; Rajca, S.; Rajca, A.; Eaton, S. S.; Eaton, G. R. Impact of Electron-Electron Spin Interaction on Electron Spin Relaxation of Nitroxide Diradicals and Tetraradical in Glassy Solvents Between 10 and 300 K. The Journal of Physical Chemistry B 2008, 112, 2818–2828.

(33) Veshtort, M.; Griffin, R. G. SPINEVOLUTION: a powerful tool for the simulation of solid and liquid state NMR experiments. *Journal of Magnetic Resonance* **2006**, *178*, 248–282.